IJST, Transactions of Civil Engineering, Vol. 39, No. C1, pp 103-123
Printed in The Islamic Republic of Iran, 2015

SEISMIC PERFORMANCE OF RC FRAMES RETROFITTED BY FRP AT JOINTS USING A FLANGE-BONDED SCHEME*

S. ZARANDI[1] AND MAHMOUD R. MAHERI[2**]

Dept. of Civil Engineering, Shiraz University, I. R. of Iran
Email: maheri@shirazu.ac.ir

Abstract– A new, FRP flange-bonded scheme, with practical application to 3D RC frames and with the aim of relocating plastic hinges away from the joints is presented and its performance is compared with that of the web-bonded scheme. For this purpose, nonlinear pushover analyses of detailed Finite Element (FE) models of retrofitted joints of a benchmark RC frame are carried out. The optimal thicknesses of the Fibre Reinforced Polymer (FRP) sheets for relocating the plastic hinges are first determined. The moment-rotation curves of the joints are then utilised to create a representing model for the RC frame. Further, nonlinear pushover analyses are carried out on the retrofitted and the original frame to evaluate their capacity curves and seismic performance parameters such as ductility, behaviour factor and performance points in relation to a specified demand earthquake. The results are then compared with those of the same frame when retrofitted with the web-bonded scheme as well as with steel bracing. Results point to the marked superiority of the flange-bonded scheme compared to the web-bonded scheme in different aspects including, capacity, ductility and the performance level and cost. The performance of the FRP flange-bonded scheme also compares well with that of the steel bracing method.

Keywords– Seismic retrofitting, RC frames, FRP, joint, nonlinear static (pushover) analysis, performance level, web-bonded, flange-bonded, steel bracing

1. INTRODUCTION

Fibre Reinforced Polymer (FRP) is widely used for seismic upgrading of existing RC structures, repairing and strengthening of damaged structures and strengthening deficient members. The seismic retrofitting of an RC frame may include strengthening members such as beams, columns and beam-column joints. Beam-column joints are critical components of a frame both in terms of structural stability and its seismic performance. FRP retrofitting of an RC beam-column joint can be performed to achieve one or more of the following objectives: (i) to enhance the shear capacity of a shear-deficient joint so that an undesirable shear (brittle) failure is changed into a more favourable flexural (ductile) failure, (ii) to enhance moment capacity and to relocate the plastic hinge away from the face of the column and further into the beam to avoid undesirable formation of plastic hinge inside the joint, and (iii) to change a weak column-strong beam behaviour into a more desirable strong column-weak beam response by enhancing column strength at the joint area. To achieve the first objective, web-bonded schemes are generally used (Fig. 1). To achieve the second objective, both web-bonded and flange-bonded schemes can be employed and the two schemes may be used together with wrapping of column sections at joint to achieve the third objective. It should be pointed out that to achieve the second objective, i.e. relocation of the plastic hinge; the web-bonded retrofitting schemes suffer from being impractical in the actual 3D frames due to the presence of cross beams and the integrated slab at the joint. They can only be effectively used to retrofit 2D frames.

*Received by the editors October 7, 2012; Accepted September 22, 2014.
**Corresponding author

A large number of studies have been carried out on FRP-retrofitted beam-column joints using a number of different retrofitting schemes. One of the earliest works dealing specifically with FRP retrofitting of RC beam-column joints was carried out by Parvin and Granata [1]. In a numerical study they investigated three different flange-bonded configurations differing only in the use of fibre wraps to avoid debonding. They noted that a large increase in the joint moment capacity, prior to formation of plastic hinge, is achieved through flange-bonded FRP overlays. Granata and Parvin [2] furthered their work through experimenting with FRP retrofitted joints. They confirmed their earlier findings regarding the increased moment capacities of the joints. Another early work is due to Mosallam [3] dealing specifically with repairing damaged RC joints with epoxy resins and FRP laminates. He concluded that the repair scheme increases the joint's strength beyond its undamaged capacity. In another experimental study, Pantelides et al. [4] tested half-scale beam-column joints retrofitted by FRP overlays and reported substantial increase in strength and improved performance regarding ductility and drift. Li et al. also tested RC joints retrofitted by hybrid FRP sheets [5]. They concluded that the hybrid FRP scheme greatly improves the stiffness and load carrying capacity of the joint and delays crack initiation at the joint through confinement due to FRP. Combined use of epoxy resin injection and FRP jacketing to rehabilitate RC beam-column joints was investigated by Karayannis and Sirkelis [6]. Their experiments showed that the use of epoxy resin can restore the strength of an even large-scale damaged joint and that application of FRP sheets provided substantial further improvements on both load-carrying capacity and ductility and that failure in the retrofitted joints occurred outside the retrofitted area.

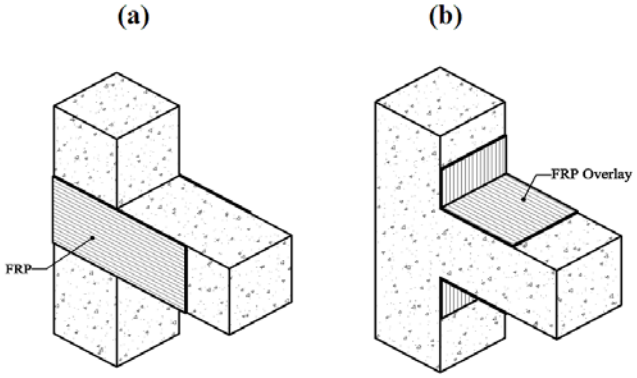

Fig. 1. Schematic representation of (a) the web-bonded and (b) flange-bonded FRP retrofitting schemes

Ghobarah and Said [7] investigated shear strengthening of non-ductile RC beam-column joints using FRP wraps. Different fibre-wrap rehabilitation schemes, including U-shaped and X-shaped configurations, were applied to pre-damaged 2D joints and assemblage was subjected to cyclic loading. They found that all the selected schemes were successful in changing the failure mode of the joint from a non-ductile shear to a ductile flexure. In 2002, Antonopoulos and Triantafillou [8] developed analytical models for the analysis of RC joints strengthened by FRP strips or sheets. Their models provide equations for stresses and strains at various stages of the response to failure by either concrete crushing or FRP fracture or debonding. They concluded that the effectiveness of the FRP retrofitting scheme increases considerably if debonding is suppressed and depends heavily on the distribution of layers in the beams and columns. Antonopoulos and Triantafillou later published the results of a series of experiments they had carried out on shear-deficient beam-column joints retrofitted by both FRP Strips and sheets [9]. In a recent paper, Le-Trung et al. [10] also investigated the performance of FRP sheets in increasing the shear capacity of a joint. They experimented on specimens representing exterior beam-column joints, retrofitted with different T-shape, L-shape, X-shape and strip configurations. The results showed noticeable improvements in joint capacity and ductility for all retrofitting schemes, particularly for the X-shaped configuration.

Appropriate FRP retrofitting schemes can also improve the performance of beam-column joints through relocating the plastic hinge away from the face of the column and further into the beam. In retrofitting an RC frame using steel X-bracing, this can readily be achieved through the connection mechanism between the bracing system and the RC frame at the beam-column intersection [11, 12]. Mahini and Ronagh [13] tested the effectiveness of FRP web-bonding of scaled beam-column RC joints in relocating the plastic hinge away from the column face. Their experimental studies showed that the FRP web-bonding scheme can restore/upgrade the integrity of the joint, keeping/upgrading its strength, stiffness and ductility, as well as shifting the plastic hinge from the column face further into the beam. The practicality and effectiveness of using web-bonded FRPs on plastic hinge relocation has also been reported by Smith and Shrestha [14]. Recent experimental work by Ravi and Arularj [15] has also shown the effectiveness of wrapping beam-column joints in changing the behaviour of a weak column-strong beam assemblage into a strong column-weak beam one by substantially increasing joint capacity and ductility. In another recent study, Niroomandi et al. [16] carried out a detailed numerical investigation into the effectiveness of FRP web-bonding of joints in relocating the plastic hinge and in enhancing the seismic performance level of an RC frame thus retrofitted. They compared the results of retrofitting the frame at joints web by FRP sheets with those obtained from retrofitting the same frame using a steel X-bracing scheme [17] and found that both retrofitting schemes have comparable abilities to increase the behaviour factor, R, of the frame; the former comparing better on the ductility component and the latter on the overstrength. They also highlighted the limitations of web-bonded scheme in relocating the plastic hinge in large beam-column joints and suggested that a combination of web-bonding and flange-bonding may be more suitable [16].

Despite the large amount of research conducted on the behaviour of different RC frame components, including joints retrofitted with FRP, little research has been carried out on the behaviour of FRP-retrofitted RC frames. In an experimental study, Balsamo et-al. [18] evaluated the seismic behaviour of a full-scale RC frame repaired using CFRP laminates. They indicated that the repaired frame had a large displacement capacity without exhibiting any loss of strength, while providing almost the same energy dissipation of the original frame. In another experimental study Di Ludovico et-al [19] carried out bi-directional seismic tests on an under-designed, full-scale RC frame and repeated the tests on the same frame after retrofitting it at joints and columns by FRP. Their experimental results showed the effectiveness of the FRP retrofitted configuration in improving the global performance of the structure in terms of ductility and energy dissipation capacity and enhancing its load capacity by 50%.

Considering the practical limitations of the current web-bonded and web-flange-bonded schemes for retrofitting RC joints, in this paper a flange-bonded scheme is introduced which can be applied to both 2D and 3D frames and also allows for the presence of slab in the joint area. The objective of the proposed flange-bonded scheme is to relocate the plastic hinge away from the face of the column to ensure that it does not occur in the joint area. It is assumed that the beams have sufficient shear capacities so that failure is ductile. The ability of the proposed configuration in achieving its objectives is compared with that of the joint web-bonded retrofitting scheme. A performance-based investigation is then carried out on an RC frame retrofitted at joints using the flange-bonded scheme and the results are compared with those reported previously for the same frame, retrofitted using the FRP web-bonded scheme [16] and a steel X-braced scheme [17]. The numerical investigations are carried out in two parts; first, nonlinear pushover analyses are conducted on detailed numerical models of the individual joints of the frame before retrofitting and after retrofitting using the ANSYS analysis software [20]. In this part, the optimal FRP laminate thickness required to successfully relocate the plastic hinge is determined through analysing each retrofitted joint with different laminate thicknesses. The response properties of the retrofitted and the original joints, in the form of moment-rotation capacity curves are then extracted from the results of

pushover analyses and used in the second part of the investigations to form an accurate numerical model of the full RC frame. Nonlinear pushover analyses are then carried out on the numerical models of the frame before and after retrofitting using the SAP2000 [21] analysis software and their respective capacity curves are obtained. The capacity curves are, in turn, utilised to extract the seismic behaviour parameters of the frames; including ductility ratio and the behaviour factor and to carry out a performance-based evaluation of the frame before and after retrofitting. Finally, the results are compared with each other and with those reported earlier using the aforementioned other retrofitting schemes.

2. CAPACITY ANALYSES OF THE FRAME JOINTS

a) The FRP flange-bonded scheme

In the flange-bonded scheme used in this study, FRP laminates are placed on the top and bottom flanges of the beams ends joining the joint and are extended so that they cover parts of the adjoining column faces. Similar to tensile steel reinforcement in RC members, the FRP overlay should have sufficient development length or anchorage so that its full design strength could be utilised. The adhesion of the composite overlay to the concrete at the column face does not by itself provide sufficient anchorage. This is because the direct tensile debonding of concrete cover at the beam-column interaction occurs at small loads. Anchoring the end of the FRP overlay to the column can be achieved effectively using FRP strips wrapped around the column as seen in Fig. 2.

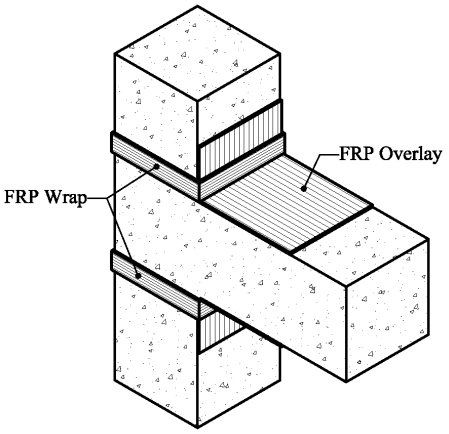

Fig. 2. Wrapping of the FRP overlay in the flange-bonded scheme

In this flange-bonded configuration, debonding may occur in two forms; first, the abovementioned debonding which may be controlled through using sufficient amount of strip wrapping and second, debonding due to shear or normal stress concentrations at the end of the FRP overlay on the face of the beam. To control the first type of debonding, a parametric study was conducted on selected joints to determine the optimum width and thickness of the strip wrapping. It was found that for the joints of the frame under study, 100mm wide strips having a thickness half that of the overlay itself is sufficient to provide the appropriate anchorage. To control the second type of debonding, in each analysis the maximum strain in the FRP laminates was checked to ensure that it is less than the limiting quantity suggested by Chen and Teng [22] and adopted by ACI 440.2-2008 [23]. The ACI 440.2 limits the effective strain in the FRP laminate ε_{fd} to prevent debonding failure as given in the following equation.

$$\varepsilon_{fd} = 0.41\sqrt{\frac{f'_c}{n.E_f.t_f}} \leq 0.9\varepsilon_{fu} \quad (1)$$

where, f'_c is the standard concrete cylinder compressive strength, E_f and t_f are the elastic modulus and the thickness of the FRP laminate, respectively, and *n* is the number of laminate layers.

b) Numerical models of the retrofitted joints

The frame used in this study is a 2D, three-bayed, eight-storey RC frame first designed and investigated when retrofitted with steel bracing by Maheri and Akbari [17]. The same frame was later used by Niroomandi et al. [16] to study the effects of retrofitting joints by FRP web-bonded scheme. In designing the moment resisting frame, the design dead and live loads were assumed to be 27.5 kN/m and 17.5 kN/m, respectively. The compressive strength, f'_c and tensile strength, f_t of concrete were taken as 27.46 MPa and 3.668 MPa, respectively. Also, the elastic modulus of the concrete, E_c, was assumed as 24.63 GPa and the yield stress of steel reinforcement was taken to be 412 MPa. Design base shears were determined for a Peak Ground Acceleration (PGA) of $0.3g$. The frame was designed based on the weak beam-strong column principle using the ACI-95 Code [24]. In that study, the steel bracing system was designed using the AISC-LRFD Code. Dimensions and flexural reinforcements of the designed beam and column sections are shown in Fig. 3. In this figure, ρ_t, ρ_s and ρ'_s are, respectively, the total steel ratio of columns and the tensile and compressive steel ratios of the beams. This moment resisting frame is used in the present study; with the flange-bonded FRP-retrofitted joints replacing the steel bracing system.

A reinforced concrete joint retrofitted by FRP is a complex composite system consisting of different materials with different properties. Therefore, developing an appropriately detailed numerical model is of prime importance. In the following, such a model is developed using the ANSYS software and its accuracy is verified using available numerical data [16].

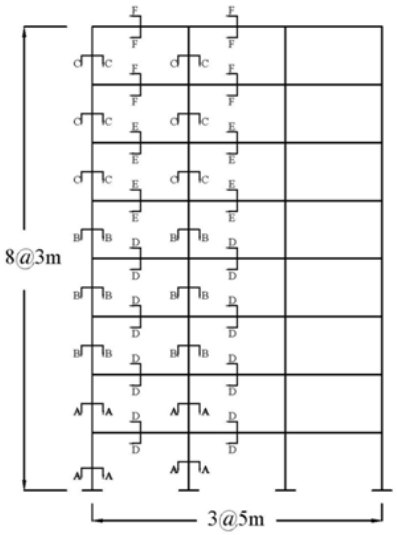

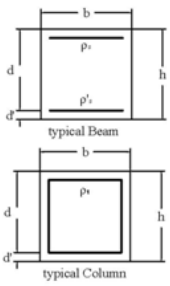

section	b	h	d	ρ_t	ρ_s	ρ'_s
A-A	700	700	650	0.019	—	—
B-B	500	500	450	0.022	—	—
C-C	500	500	450	0.013	—	—
D-D	500	500	450	—	0.012	0.009
E-E	500	500	450	—	0.011	0.0071
F-F	500	500	450	—	0.0071	0.004

Fig. 3. The reference moment resisting frame [16]

In the FE numerical models of the joints, concrete was modelled using an eight-node solid element, specially designed for concrete material (ANSYS element solid65). This element is capable of handling plasticity, creep, cracking in tension and crushing in compression. The 5-parameter William-Varnk model was used as the failure criterion. This model allows for the cracking of concrete in tension and crushing of concrete in compression and uses a smeared crack model [20]. The longitudinal and transverse reinforcements were modelled individually using two-node link elements (ANSYS element link8). A bi-linear curve with 2% post yield strain hardening was used to represent the stress-strain relation for steel. The FRP overlays and wrapping strips were modelled using the eight-node, three-dimensional, multi-layered solid element; denoted as solid46 in ANSYS software. This element has translational stiffness but

no bending stiffness. It also uses an anisotropic material. The material uses a linear stress-strain curve in both compression and tension and in any of the Cartesian directions. In a preliminary investigation carried out by the authors, it was found that, due to its multi-layered nature, the element solid46 produces better results than the element solid45 used previously to represent FRP laminates by some researchers [1, 16, 25]. The material properties assigned to the FRP laminates are the same as those used in reference [16].

The geometry of each joint in the numerical models is taken as to include half the length of the beams and columns joining the connection. The finite element mesh of a typical internal joint retrofitted using the flange-bonded scheme is shown in Fig. 4. The number of elements used to model this joint include 4980 Solid65 (concrete) elements, 1764 Link8 (steel bar) elements and 336 Solid46 (FRP) elements. Representing boundary conditions were applied to the columns ends, so that the columns constant axial compression force at the joint could be applied throughout the analysis. To perform the nonlinear pushover analyses on the external joints, the stepwise load was applied downwards at the tip of the beam, whereas for the internal joints, equal and opposite loads were applied to the beams ends as shown in Fig. 5. In the nonlinear finite element model, both geometric and material nonlinearities were taken into account. The solution to the nonlinear pushover problem was carried out using the modified Newton-Raphson method.

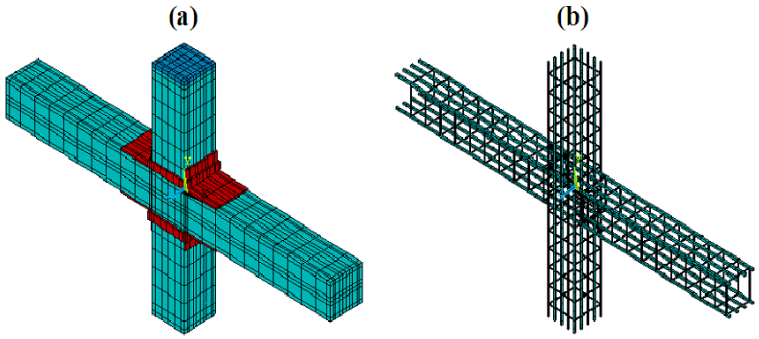

Fig. 4. The FE representation of a typical internal joint (a) concrete and FRP elements and (b) steel reinforcement

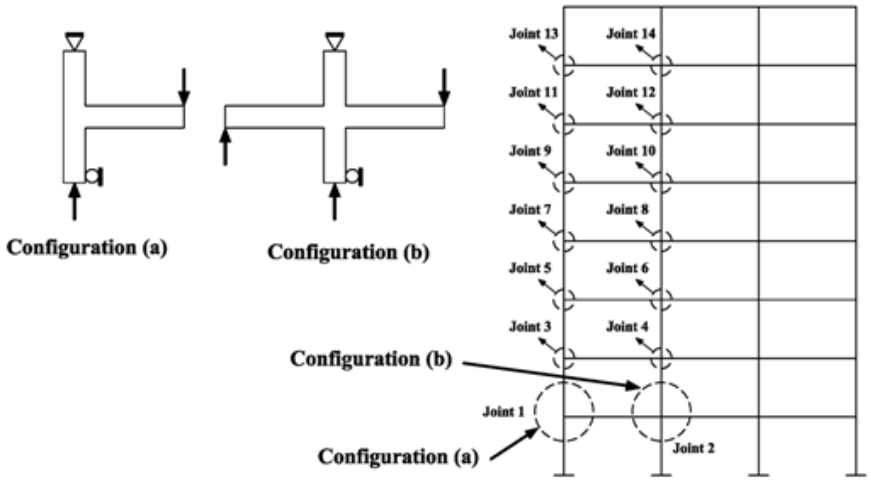

Fig. 5. Selected joints of the frame and the assumed loading and boundary condition configurations for pushover analysis

To verify the reliability of the joints numerical models, a typical joint (joint 13) of the 2D frame investigated by Niroomandi et al [16] was selected and retrofitted by FRP on its web, in the same manner

as that carried out in reference [16]. The only difference between the two numerical models was the type of ANSYS element used to represent the FRP laminates; being element SOLID45 in that reference. Figure 6 compares the moment-rotation curves extracted from the nonlinear pushover analyses of the two studies. The two curves compare well, indicating the reliability of the numerical models used in this study.

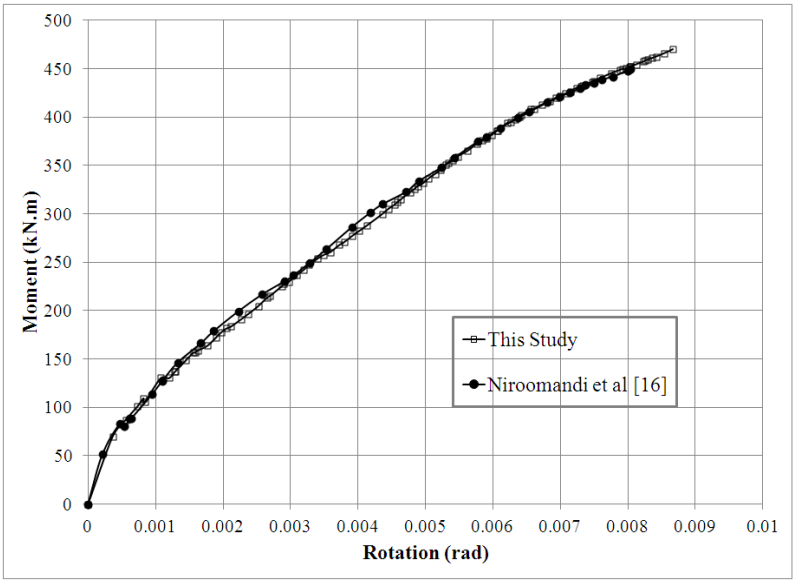

Fig. 6. Comparison of the results on the web-bonded joint 13

c) Pushover analyses of the retrofitted joints

To retrofit an RC frame, the number of FRP layers required to successfully relocate the plastic hinge away from the face of the column needs to be determined for every joint in that frame. For each joint of the frame under consideration, therefore, nonlinear pushover analysis of the joint was performed using different FRP thicknesses and for each thickness the state of strain in the tensile reinforcements of the beam was used to determine the position of plastic hinge. The length of FRP sheets was kept constant as 500mm for all joints based on the Pauley and Priestly [26] design approach for obtaining the desirable plastic hinge relocation. As a typical example, the maximum strain variation in the longitudinal tensile reinforcements of the beam joining the external joint No. 1 (Fig. 5), retrofitted with 4, 5 and 8 layers of FRP laminates, corresponding respectively to thicknesses of 0.66mm, 0.825mm and 1.32mm, are compared with the reinforcement strain variation in the original (non-retrofitted) beam in Fig. 7. As it is evident in this figure, for the original model the maximum reinforcement strain, corresponding to the location of plastic hinge, expectedly occurs close to the column face. When the joint is retrofitted with 4 layers of laminates, it can be seen that there are two peaks, one at the column face and the other at the end of FRP laminates. Because the two peaks are close in values it is assumed that a safe relocation has not occurred. However, when the joint is retrofitted with 5 layers of laminate, the amplitude of the peak at the end of FRP overlay clearly dominates the peak formed at the column face; indicating a successful relocation of the plastic hinge to the end of overlay. Larger thicknesses of FRP, such as the case of 8 layers shown in Fig. 7, although showing similar abilities for relocation, would naturally be uneconomical. Therefore, for this joint a 5-layer overlay is considered as the optimal thickness for successful plastic hinge relocation.

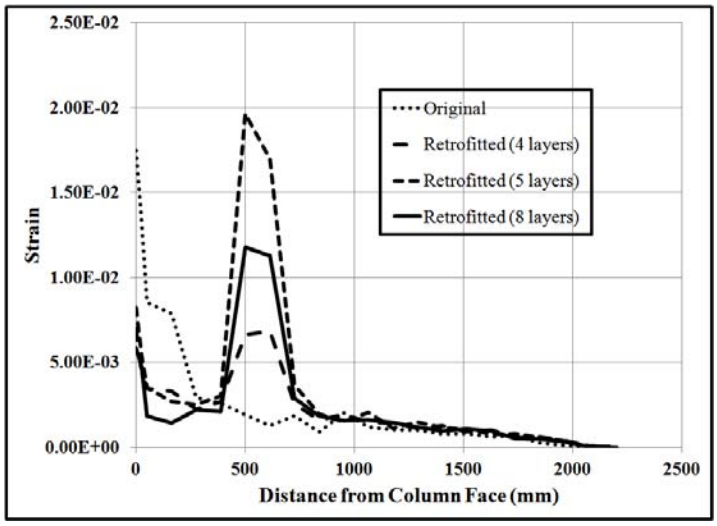

Fig. 7. The maximum strain variation in the tensile reinforcements of the beam joining external joint 1

Similarly, Fig. 8 shows the maximum strain variation in the longitudinal reinforcements of the two beams joining a typical internal joint (joint No. 6). In Fig. 8a, in which the state of strain in the left beam of the joint is shown, it can be seen that 7 layers of laminate are necessary for successful relocation of the plastic hinge in this beam. However, Fig. 8b shows that the same thickness of overlay does not relocate the plastic hinge in the more heavily reinforced right beam. For plastic hinge relocation in this beam, 9 layers would be required. The results of the nonlinear pushover analyses of all joints are summarised in Table 1.

Table 1. Retrofitting details and strength and ductility properties of the joints

Joint	Side	No. of FRP layers	Moment Capacity (M_{max}) (kN.m)			Ductility (μ)		
			Original	Retrofitted	% Difference	Original	Retrofitted	% Difference
13	R	3	407	481	18	21.5	13.4	-37
11	R	7	424	653	54	11.6	22.0	89
9	R	5	452	664	49	10.2	15.5	52
7	R	6	474	708	49	9.5	14.4	51
5	R	7	510	686	34	16.8	22.2	32
3	R	5	518	653	26	22.5	17.1	-24
1	R	5	518	653	26	22.5	17.1	-24
14	L	4	190	253	33	23.2	25.0	8
	R	4	306	445	45	22.6	26.4	17
12	L	6	262	364	39	19.5	25.5	30
	R	7	343	456	33	18.5	24.5	32
10	L	7	159	379	138	6.0	17.0	183
	R	10	-	-	-	-	-	-
8	L	11	209.8	462.2	121	3.75	12.8	241
	R	12	-	-	-	-	-	-
6	L	7	303	467	54	9.8	13.1	33
	R	9	378	600	58	15.2	24.5	61
4	L	5	-	-	-	-	-	-
	R	5	495	640	29	20	22.0	10
2	L	5	-	-	-	-	-	-
	R	5	495	640	29	20	22.0	10

R = Right beam, L = Left beam

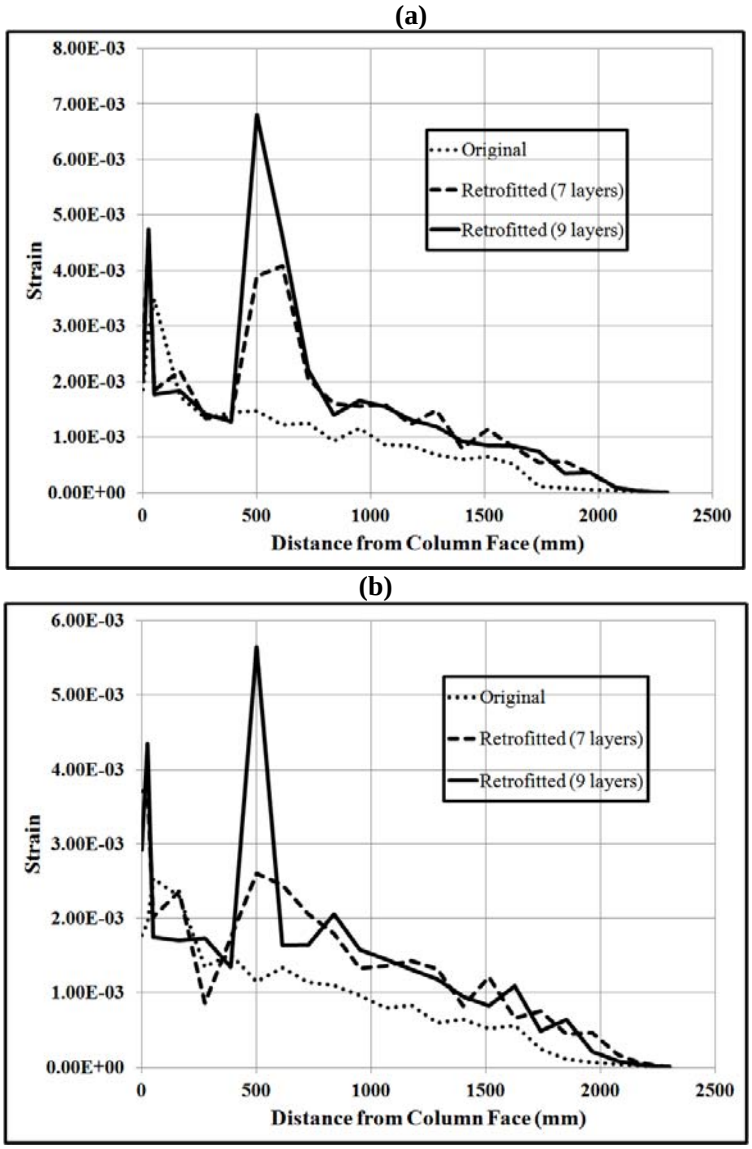

Fig. 8. The maximum strain variation in the tensile reinforcements of the (a) left beam and (b) right beam joining internal joint 6

Regarding the term "successful relocation", four further points should be taken into consideration, as follows:

1) Plastic hinging inside the beam: To ascertain a weak beam-strong column performance in the joints, the state of strain in the longitudinal bars of the columns were monitored and compared with that of the beams. It was found that for all the joints, the plastic hinge occurred in the beams and not the columns.

2) Location of the first reinforcement yield: To ensure that the location of the maximum strain in the beam tensile reinforcement corresponds to the location of the first reinforcement yield, the location of the latter was extracted from the pushover results and it was found that in all the retrofitted joints the location of the maximum strain indeed corresponds to the location of the first yield.

3) Control of debonding: As it was stated previously, debonding may occur at the column face and/or at the end of FRP overlay on the beam. The first type of debonding is avoided by using an appropriate amount of FRP strip wrapping. The state of concrete tensile strain at this location would not be critical as the wrapping provides sufficient anchorage. However, the maximum concrete strain at the end of FRP

overlay was extracted from the analysis results and checked against the limiting strain given in Eq. (1). It was found that for the lighter joints (the joints requiring smaller number of FRP layers) the state of concrete strain satisfies the limiting strain, however, for some stronger joints debonding may occur prior to the plastic hinge ultimate capacity. This, however, does not mean that relocation cannot occur for such joints; it merely states that the full potential of the plastic joint may not be utilised prior to debonding. Therefore, anchoring the end of FRP overlay may become necessary for some joints. Figure 9 shows a 3D view of the state of concrete strain in a typical internal joint, before and after retrofitting. Relocation of the plastic hinges in the retrofitted case may be deduced from the areas of high strain concentrations.

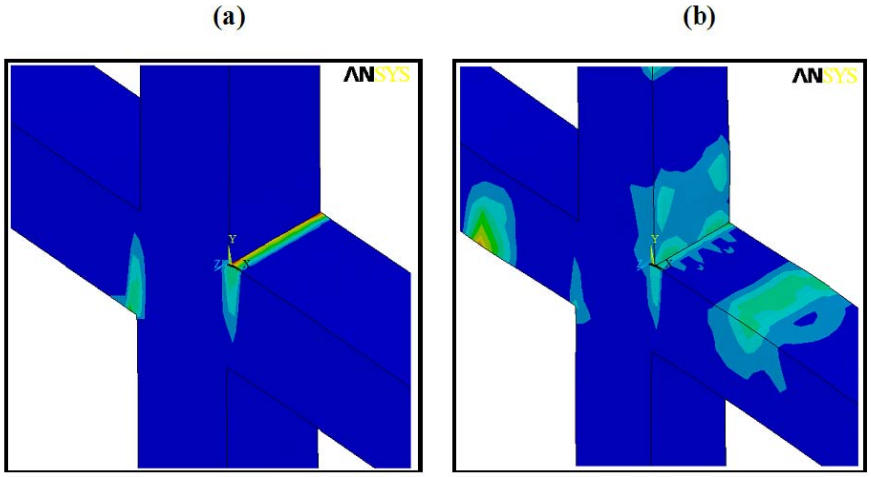

Fig. 9. Schematic view of the strain distribution in concrete material of the internal joint 14

4) The ability of a plastic hinge to perform well by ductile rotation also depends on the state of concrete compressive strains. Since FRP overlays do not work in compression, the critical location to monitor the state of concrete compressive strain would be at the column face, rather than the location of plastic hinge. The state of concrete compressive strain would be automatically monitored by the ANSYS software and the analysis would be stopped when the maximum strain reaches the limiting strain if in the concrete material section the option "crash on" is activated. However, if this option is not activated, the state of concrete strain should be monitored manually after the analysis and if the limiting strain is violated, the capacity curve beyond the point of compressive failure should be discarded. In the present study, initially both options were used for some joints for the purpose of comparison but the curves obtained using the "crash on" option are used to further the investigations. A look at the state of concrete compressive strains shows that due to inherent ductility in the original RC frame under investigation, crashing of concrete did not occur in any joints and all failures were as a result of excessive straining of the tensile reinforcements. If the original joints are of limited ductility, appropriate provisions would be required to upgrade the compressive strength of the beam.

The force-beam tip vertical displacement curves obtained from the nonlinear pushover analyses for the retrofitted and the original joints were converted to moment-rotation curves. Moment-rotation curves of the original and the retrofitted joint No.11, as a typical example, are compared in Fig. 10. The ability of the flange-bonded retrofitting scheme in enhancing both the capacity and ductility may be deduced from these curves. The effects of retrofitting scheme on the moment capacity and the rotational ductility of all the joints are highlighted in Table 1. Increases ranging from 18% to 138% for the moment capacity and from 8% to 241% for ductility are noted due to the retrofitting scheme.

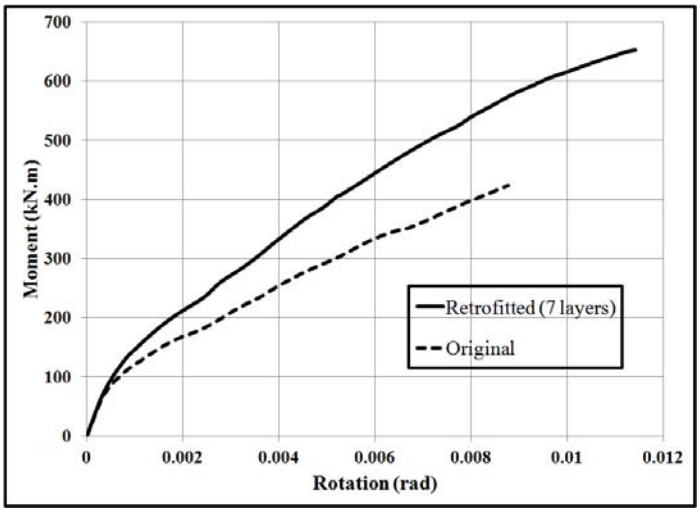

Fig. 10. Moment-rotation curves for the external joint 11

3. SEISMIC PERFORMANCE PARAMETERS OF THE FULL FRAME

a) Nonlinear pushover analyses of the full frame

In the second phase of studies, nonlinear pushover analyses are conducted on the original and the retrofitted full RC frame under investigation using the SAP2000 numerical analysis software. The FE model of the frame is shown in Fig. 11. In this model, the contributions of the flange-bonded overlays to the rotational stiffness (*Ki*) of the retrofitted joints, evaluated from the moment-rotation capacity curves in the previous section, are modelled as nonlinear rotational link elements (NLLink). These elements are assumed to be located at a distance of 500mm away from the column face, corresponding to the length of the FRP overlay. Nonlinear elements capable of modelling plastic hinging are used for the ends of the beams and columns. Flexural moment hinges are assigned to the ends of the beams, while axial-moment hinges are assigned to the ends of columns. Force-deformation criteria for plastic hinging is defined based on the ATC-40 [27] and FEMA356 [28] patterns. Prior to the incremental application of the lateral load, a constant gravity load equal to the total dead load plus 20 percent of the live load, was applied to each frame.

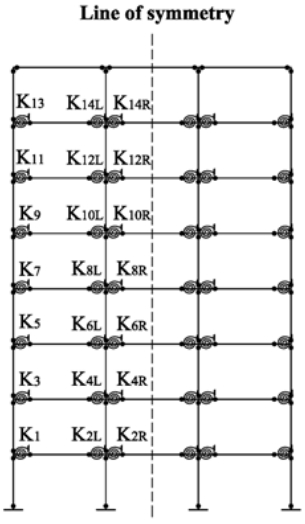

Fig. 11. The FE model of the full frame for the nonlinear pushover analyses in SAP2000

In a nonlinear pushover analysis, lateral forces should be applied to the building using distributions or profiles that represent the likely distribution of inertial forces in the design earthquake. In a study by Mwafy and Elnashai [29] it was shown that for small to medium rise frames, the inverted triangular distribution of load, corresponding to the first mode of vibration, produces a better estimate of the capacity curve compared with the uniform distribution and is more practical than a multi-modal distribution. As a result, an inverted triangular distribution over the height is used as the lateral load pattern. P-Δ effect is also considered in the analysis. The base shear versus roof displacement curves for the original and the retrofitted frame, obtained from the pushover analyses, are compared in Fig. 12. As it is shown, the flange-bonded FRP-strengthening of the joints resulted in an increase of around 160% in the ultimate lateral load carrying capacity of the RC frame. This substantial increase is due to a number of factors including: change in the response of the frame from weak column-strong beam to weak beam-strong column, increased rotational stiffness of the joints due to flange-bonded FRP and particularly, the increased stiffness of the beams due to plastic hinge relocation, in effect reducing the effective length of the beams.

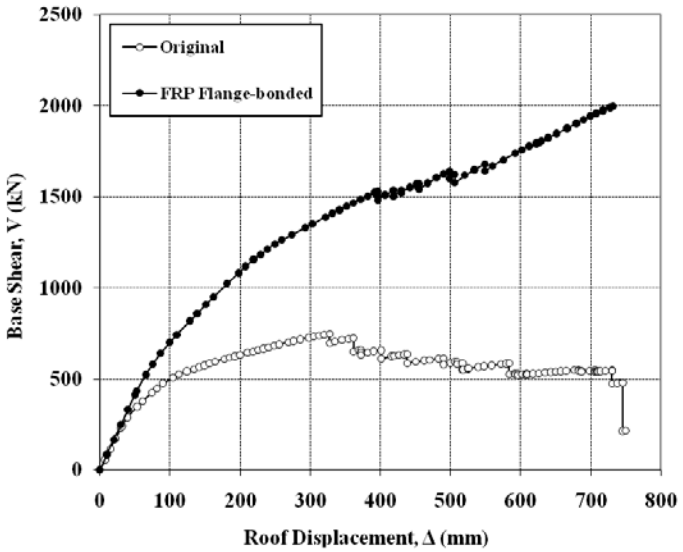

Fig. 12. Pushover capacity curves for the retrofitted and the original frames

b) Seismic behaviour parameters

In forced-based seismic design procedures, seismic behaviour factor, R, is a force reduction factor used to reduce the linear elastic response spectra to the inelastic response spectra. In other words, seismic behaviour factor is the ratio of the strength required to maintain the structure elastic to the inelastic strength of the structure [17]. For structures designed using an ultimate strength method, the seismic behaviour factor, R, is expressed in the following form,

$$R = R_{\mu}.R_{s} \tag{2}$$

where, R_{μ} is the ductility-dependent component, also known as the ductility reduction factor and R_s is the overstrength factor.

With reference to Fig. 13, in which the actual force–displacement response curve is idealized by a bilinear response curve, the seismic behaviour factor parameters may be defined as:

$$R_{\mu} = V_e / V_y \, , R_s = V_y / V_s \tag{3}$$

where, V_e, V_y and V_s denote the elastic response strength of the structure, the idealized yield strength and the first significant yield strength, respectively.

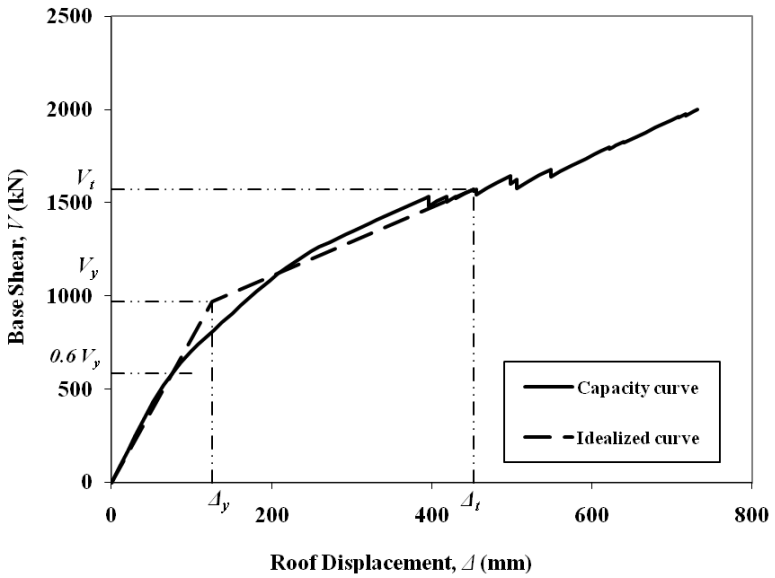

Fig. 13. Bilinear idealisation of the capacity curve for evaluation of seismic behaviour parameters

Ductility reduction factor, R_μ, is a function of the characteristics of the structure, including ductility, damping and fundamental period of vibration, T, as well as the characteristics of earthquake ground motion. Therefore, it cannot be directly evaluated from the relation given in Eq. (3), as the elastic response strength, V_e, itself is a dependent variable. Many investigators have presented relations for evaluating the ductility reduction factor, amongst which the relation given by Nassar and Krawinkler [30] is the most representing [17]. They state that:

$$R_\mu = \left[c(\mu - 1) + 1\right]^{1/c} \tag{4}$$

where,

$$c(T, \alpha) = \frac{T^a}{1 + T^a} + \frac{b}{T} \tag{5}$$

In Eq. (4), μ is the structure ductility ratio, defined in terms of the ratio of the maximum structural displacement Δ_{max}, to the displacement corresponding to the idealized yield strength, Δ_y. In Eqn. 5, α, is the post-yield stiffness given as a percentage of the initial stiffness of the system and a and b are parameters given as functions of α [30].

The maximum displacement may be considered as the displacement corresponding to the maximum load (in a force-controlled analysis) or a code-specified target displacement, Δ_t. Different codes specify different values for Δ_t ranging from 1% to 3% of the height of the building. The NEHRP guidelines [31] indicate that, for a specific earthquake, the building should have enough capacity to withstand a specified roof displacement. This is called the target displacement and is defined as an estimate of the likely building roof displacement in the design earthquake. The guidelines present the following expression to estimate the target displacement [31]:

$$\Delta_t = C_0 C_1 C_2 C_3 S_a \frac{T_e^2}{4\pi_2} g \tag{6}$$

where, the modification factors C_0, C_1, C_2 and C_3 relate, respectively, to the spectral displacement and expected maximum elastic displacement at the roof level; the expected maximum inelastic displacements to displacements calculated for linear elastic response; the effects of stiffness degradation, strength

deterioration, and pinching on the maximum displacement response and the increased displacements due to dynamic second order effects. Also, T_e, represents the effective fundamental period of the building in the direction under consideration, calculated using the secant stiffness at a base shear force equal to 60% of the yield force and S_a is the response spectrum acceleration at the effective fundamental period and damping ratio of the building.

To determine the equivalent structural yield displacement, Δ_y, and yield strength, V_y, the idealized bilinear force-displacement capacity curve for each frame was evaluated based on the method recommended by FEMA-356 provisions. With reference to Fig. 13, line segments on the capacity curve were located using a procedure that approximately balances the area above and below the curve. The effective lateral stiffness, K_e, was also taken as the secant stiffness calculated at a base shear force equal to 60% of the effective yield strength of the structure [31].

After evaluating the ductility ratio, μ, and the equivalent yield strength, V_y, the ductility reduction factor, R_μ can be obtained from Eqns. 4 and 5 and the overstrength factor, R_s is determined from Eq. (3). The seismic behaviour factor parameters for the original and the retrofitted frames were thus calculated and are presented in Table 2. Also presented in this Table are the corresponding results reported previously for the same frame retrofitted using the FRP web-bonded scheme [16] and retrofitted by steel concentric X-bracing [17].

Table 2. The seismic behaviour parameters of the frames

Frame		Δ_t (mm)	μ	R_μ	R_s	R
Original	$\Delta_{max} = \Delta_t$	510	2.27	2.4	1.9	4.6
FRP Flange-bonded	$\Delta_{max} = \Delta_t$	452	3.58	4.1	2.4	9.8
	$\Delta_{max} = 0.015h$		2.84	3.1	2.4	7.4
FRP Web-bonded [16]	$\Delta_{max} = 0.015h$	472	2.83	3.0	3.2	9.6
Steel X-braced [17]	$\Delta_{max} = 0.015h$	-	2.70	2.66	2.97	7.9

Table 2 shows that the flange-bonded retrofitting scheme has increased the ductility ratio, μ, of the original frame by 57%. The ductility ratios for the frames retrofitted with the flange-bonded and web-bonded schemes are effectively the same; however, they are somewhat more than the frame retrofitted with steel bracing. The overstrength factor (R_s) for both the web-bonded scheme and the steel bracing method are higher than the flange-bonded scheme. This is because in the web-bonded scheme, the first plastic hinge (V_s) is formed at a much earlier stage compared to the flange-bonded scheme, and in the frame retrofitted with steel bracing, the global yield (V_y) is much higher than the flange-bonded scheme. Taking all the above factors into consideration, we can see that the behaviour factor of the flange-bonded retrofitting scheme and the X bracing method are almost the same, whereas the frame retrofitted with the web-bonded scheme has a higher behaviour factor than these two methods. However, when compared to the original frame, all three retrofitting methods result in substantial increases in the behaviour factor of the frame.

c) Seismic performance levels

In a performance-based design or evaluation, the seismic performance level of a structure describes its state of damage on a capacity spectrum curve. To evaluate the seismic performance of the structure, the nonlinear base shear-roof displacement capacity curve of the structure is first determined using any of the static (pushover), cyclic or dynamic methods. The capacity curve is then converted to the 'capacity' Acceleration-Displacement Response Spectrum (ADRS) curve (S_a-S_d) and its performance level in relation to a specific, code-recommended, ADRS 'demand' curve is obtained using the instructions provided by ATC-40 [27], where, S_a and S_d are the spectral acceleration and displacement, respectively. Figure 14,

shows how the performance point of the FRP-retrofitted frame is obtained using these instructions. In this figure, the capacity ADRS curve is compared with the demand ADRS curve provided by the Iranian seismic code [32] for a design base acceleration (A) of 0.25g and 5% elastic response damping. Considering that the actual damping of the structure undergoing inelastic response is far in excess of the assumed elastic damping of the demand ADRS, appropriate modification to the demand ADRS curve is necessary. Such modification may be carried out using an iterative procedure based on the guidelines given in [27] and shown in Fig. 14. In this figure, β_{eff} is the effective inelastic damping of the frame and the 'banana-shaped' curve relates to the iterative procedure used to evaluate the demand ADRS curve corresponding to the effective inelastic damping [27]. The performance point of the structure in relation to the demand earthquake is then considered as the point of intersection of the capacity and the demand ADRS curves. To evaluate the performance level of a structure, its capacity curve is first idealised by a multi-linear curve similar to that shown in Fig. 15. Each line segment of the curve represents a performance region and any point on the curve may represent a performance level. Key performance levels for a seismic performance-based design or retrofitting include: Immediate Occupancy (IO), Life Safety (LS) and Collapse Prevention (CP) (Fig. 15).

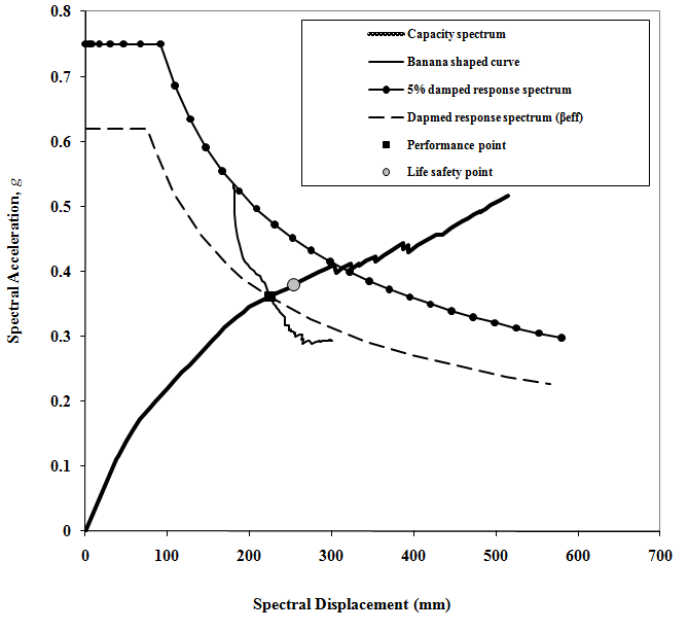

Fig. 14. Procedure to evaluate the performance point on an ADRS capacity-demand diagram

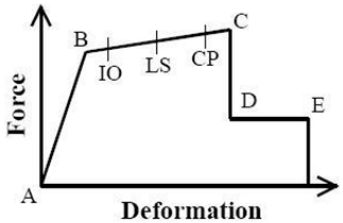

Fig. 15. Seismic performance levels on an idealised response curve

The capacity and demand ADRS curves and the performance points for the original frame and the frame retrofitted with the FRP flange-bonded scheme were evaluated in the manner described above and are shown in Fig. 16. The performance point coordinates of the frames are also listed in Table 3.

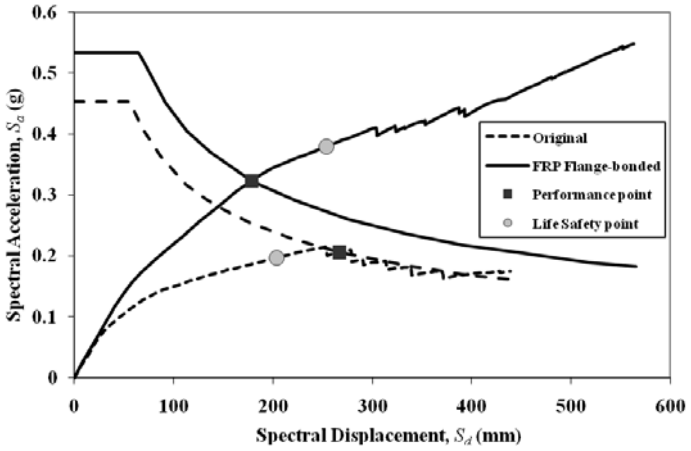

Fig. 16. Performance points of the original frame and the flange-bonded retrofitted frame in a demand earthquake with A=0.25g

Table 3. Performance point coordinates of the frames

Frame	Frame Performance Point		Performance Point for Life Safety (LS)	
	S_a (g)	S_d (mm)	S_a (g)	S_d (mm)
Original (A=0.25g)	0.206	267	0.197	204
FRP Flange-bonded (A=0.25g)	0.323	179	0.379	254
FRP Flange-bonded (A=0.30g)	0.361	225	0.379	254
FRP Web-bonded (A=0.25g) [16]	0.263	212	0.269	223
Steel X-braced with 100% share of braces (A=0.25g) [16]	0.493	65	0.579	189

With reference to Fig. 16, it is clear that the original frame does not meet the Life Safety requirement of the demand earthquake (A=0.25g), as its performance point falls short of the LS point; whereas, the retrofitted frame easily satisfies the LS requirement. The retrofitted frame not only satisfies the LS requirement for this demand earthquake, but also satisfies the LS requirement for a stronger demand earthquake with a design base acceleration of A=0.30g, as it can be seen in Fig. 17.

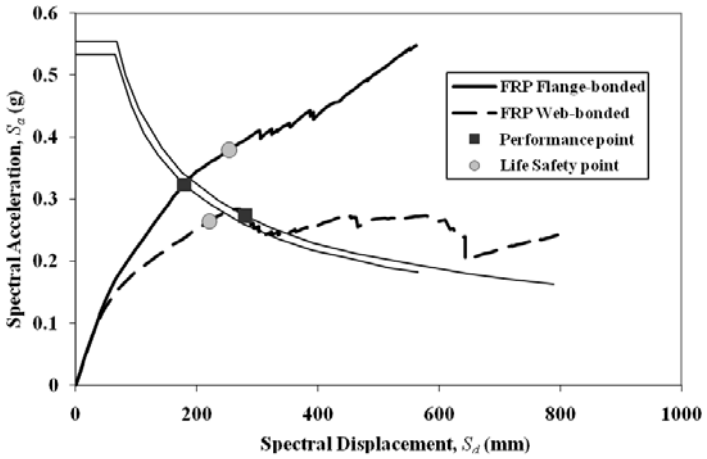

Fig. 17. Performance points of the web-bonded and the flange-bonded retrofitted frames in a demand earthquake of A=0.30g

In order for the seismic performance of the flange-bonded scheme to be compared with the performance of the other retrofitting schemes, the capacity and demand ADRS curves and performance

points (demand earthquake A=0.25g) of the original frame and the frame retrofitted with different schemes are plotted in Fig. 18 and their performance points are listed in Table 3. Comparing the capacity curves of the flange-bonded and the web-bonded FRP retrofitting schemes, it is clear that the flange-bonded scheme shows superiority, not only in terms of increased strength and ductility, but also the seismic performance level. For the flange-bonded scheme, the performance point relates to a spectral displacement of 179 mm; whereas that of the web-bonded scheme has a spectral displacement of 212 mm. The lower spectral displacement for the flange-bonded scheme indicates that the inelastic lateral load resistance has been enhanced compared to the web-bonded scheme. Also, the marked difference in the spectral acceleration values for the two schemes (23%) shows that the seismic load capacity of the flange-bonded scheme is much more than the web-bonded scheme. Furthermore, with reference to Fig. 17, it is noted that while the frame retrofitted with the flange-bonded scheme satisfies the LS requirement for the demand earthquake having A=0.3g, the same is not true for the web-bonded scheme.

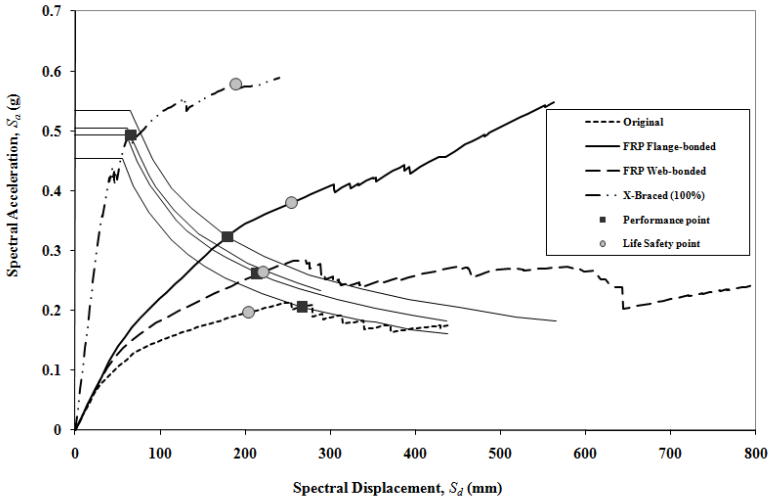

Fig. 18. Comparison between the performances of the original frame and the frame retrofitted with the FRP flange-bonded, web-bonded and the steel X-braced retrofitted frames

Comparing the seismic performances of the frame retrofitted with the FRP flange-bonded scheme and retrofitted with steel bracing, it is evident that the reduction in the spectral displacement, corresponding to an increase in the inelastic lateral capacity, is more profound in the latter retrofitting scheme. The large difference between the lateral load resistance of the steel braced frame compared with the flange-bonded FRP retrofitted frame is expected, as the strong bracing system was specifically designed to increase the stiffness and the lateral strength capacity of the RC frame [17], whereas the flange-bonded FRP retrofitting of the frame at joints was designed to increase joints rotation capacities, relocate the plastic hinges and, in general, was designed to improve the seismic performance of the frame. On the seismic performance of the two retrofitting methods, Fig. 18 indicates that both methods satisfy the LS requirement of the design earthquake in an almost equal capacity; which when we compare the relative cost of the two retrofitting methods, the FRP flange-bonded method appears to be the more attractive.

To further evaluate the effectiveness of the FRP retrofitting of the joints at flanges compared to that of the original and the other retrofitting methods, the plastic hinge distributions and their performance levels for the original and the FRP-retrofitted frames at the target displacement point and for the steel braced frame at the collapse displacement are shown in Fig. 19. In this figure, the letters A to E and notations IO, LS and CP represent the performance state of the joints as was indicated graphically in Fig. 15. The number of plastic hinges at different performance levels is also given in Table 4.

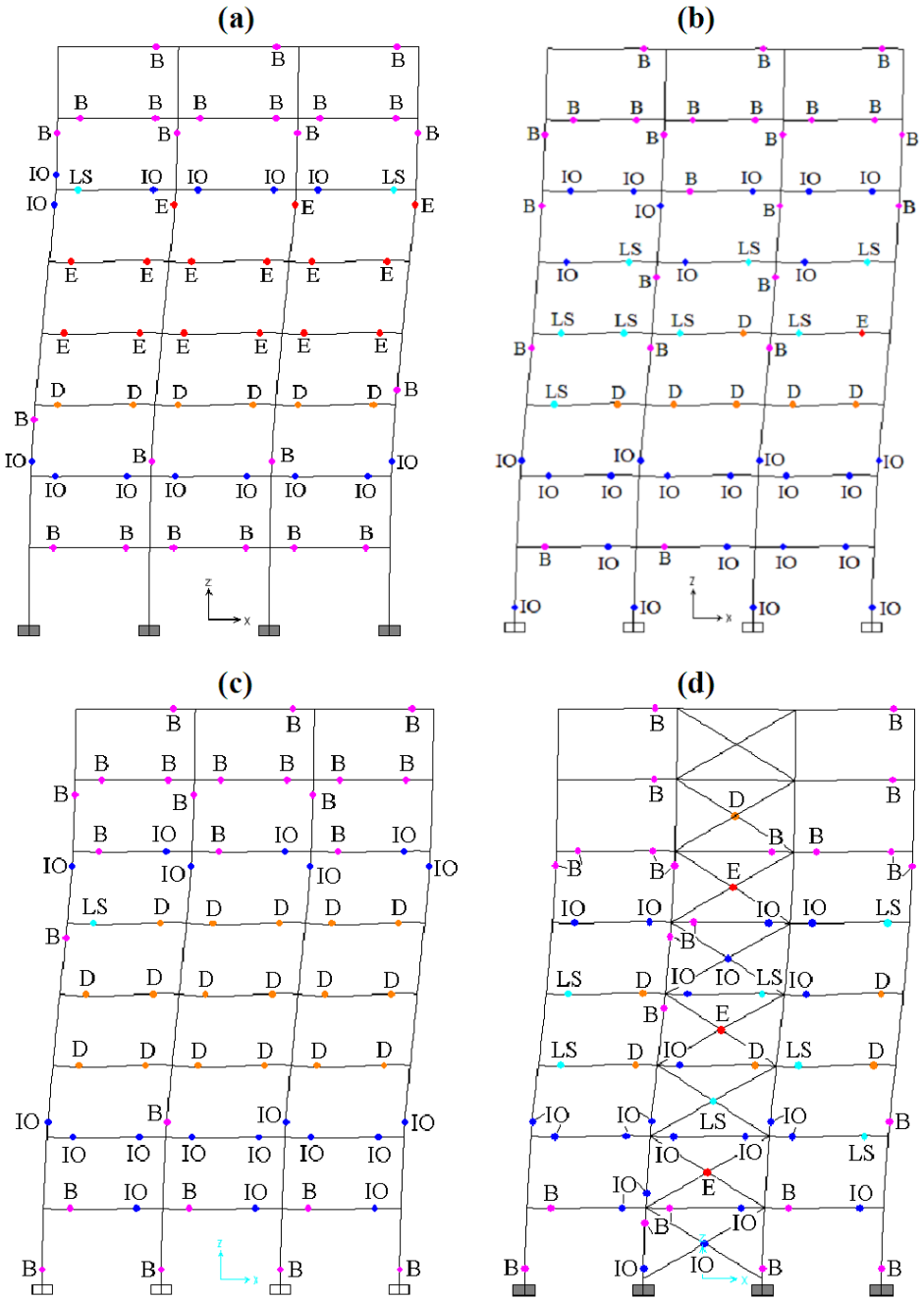

Fig. 19. Plastic hinges distribution and their performance levels in a demand earthquake of A=0.25g in (a) original frame, (b) frame retrofitted at joints flanges, (c) frame retrofitted at joints webs and (d) frame retrofitted by steel X-bracing (For notations see Fig. 15)

Table 4. Performance level of plastic hinges in the frame members

Frame	No. of plastic hinges with Performance Level of:					Total No. of plastic hinges	No. of plastic hinges not satisfying LS
	B	IO	LS	D	E		
Original	23	14	2	6	15	60	21
FRP Flange-bonded	24	27	8	6	1	66	7
FRP Web-bonded [16]	24	19	1	17	0	61	17
Steel X-braced with 100% share of braces [16]	23	22	7	6	3	61	9

In the original frame (Fig. 19a), the values of the plastic hinge rotations in the columns of the sixth floor indicate that the state of these hinges lay between points D and E on the idealised performance curve. This means that the columns in this floor will collapse during the design earthquake. However, after FRP-retrofitting the joints, by either flange-bonded or web-bonded schemes, the resulting smaller plastic hinge rotations place these column hinges in the IO-LS range (Figs. 19b and 19c). A similar shift in the state of the column hinges at the sixth floor can be achieved when the frame is retrofitted with steel bracing (Fig. 19d). Regarding the beams, Fig. 19 shows that the beams in the third, the fourth and the fifth floors do not satisfy the LS demand. The same is true for the FRP web-bonded scheme. However, marked improvements in the performances of the beams in the fourth and the fifth floors can be seen for the FRP flange-bonded and the steel braced frames; only the beams of the third floor perform less than the LS level. Comparing the state of plastic hinges in the flange-bonded scheme and the steel bracing scheme, it is interesting to note that all the bracing elements in the steel braced frame undergo large inelastic deformations, presumably due to compression buckling, so that they pass the LS level at a relatively early stage. This causes the FRP flange-bonded scheme to fare better than the steel bracing method in the number of total plastic hinges passing the LS level (Table 4).

A final point on the merit of the flange-bonded scheme is that it is far cheaper than the web-bonded scheme. Niroomandi et al. [16] reported that, for the frame under investigation to successfully relocate the plastic hinges in different joints, 10 to 30 layers of FRP laminates would be required, whereas in the flange-bonded scheme presented here, the number of layers used for the same purpose ranges from 3 to 11. The clear advantage of the flange-bonded scheme regarding cost is augmented by the fact that there is a practical limitation on the number of FRP layers which could effectively be applied, as well as the reduced effectiveness of the retrofit as the number of layers increase.

5. CONCLUSION

An FRP flange-bonded scheme is presented for retrofitting beam-column joints of RC frames specifically designed to relocate the beam plastic hinges away from the face of column to an appropriate distance into the beam. The main conclusions drawn from comparing the performance of the frame retrofitted with this method and that of the original frame and the frame retrofitted by other methods are summarised below.

1. The flange-bonded scheme is practical and can be applied to actual 3D frames as it takes into account the presence of the cross beams and the integrated floor slab, whereas for the purpose of relocating a plastic hinge, the web-bonded scheme can only be effectively applied to 2D frames.
2. The flange-bonded scheme is also more advantageous regarding the cost as it requires smaller amount of FRP material compared to the web-bonded scheme.
3. Flange-bonded FRP laminates substantially increase moment capacity and ductility of an RC beam-column joint. For the joints of frame under investigation, increases range, respectively, from 18% to 138% and from 8% to 241%.
4. Retrofitting the joints of an RC frame at beam flanges by FRP laminates can effectively relocate the beam plastic hinges away from the face of the columns. It can also greatly enhance the lateral load resisting capacity, ductility and behaviour factor of the frame. For the frame under investigation, the increases are, respectively, 166%, 57% and 113%.
5. Retrofitting joints at flanges by FRP greatly enhances the seismic performance point of the frame. A frame failing the Life Safety requirement for a demand earthquake with A=0.25g was retrofitted to pass not only the LS requirement for this earthquake, but also the LS requirement for a stronger demand earthquake with A=0.30g.

6. Seismic performance of the flange-bonded scheme far outweighs that of the web-bonded scheme. Substantial differences in the lateral load resisting capacity and ductility, as well as the performance level of the two schemes are noted. While the frame retrofitted with the flange-bonded scheme could satisfy the LS requirement of a demand earthquake having A=0.30g, the same is not true for the frame retrofitted with the web-bonded scheme. Only the behaviour factor of the frame retrofitted with the web-bonded scheme is higher than that of the flange-bonded scheme as in the case of the former, early formation of the first plastic hinge results in increased overstrength.
7. The behaviour factor for the frame retrofitted with the flange-bonded scheme is almost the same as that for the frame retrofitted with steel X bracing; the former faring better on ductility and the latter showing higher overstrength. The performance levels of the two retrofitting methods also compare well both being much higher than the web-bonded scheme. The lateral load resisting capacity of the steel-braced frame is expectedly higher than the flange-bonded retrofitting scheme, as the former is specifically designed to increase lateral capacity while the latter is designed to improve seismic performance.

REFERENCES

1. Parvin, A. & Granata, P. (2000). Investigation on the effects of fiber composites at concrete joints. *Composites, part B: Engineering*, Vol. 31, pp. 499-509.
2. Granata, P. & Parvin, A. (2001). An experimental study on kevlar strengthening of beam-column connections. *Composite Structures*, Vol. 53, No. 2, pp. 163-171.
3. Mosallam, A. S. (2000). Strength and ductility of reinforced concrete moment frame connections strengthened with quasi-isotropic laminates. *Composites, Part B: Engineering*, Vol. 31, No. 6-7, pp. 481-497.
4. Pantelides, C. Clyde, C. & Reaeley, L. (2000). Rehabilitation of R/C building joints with FRP composites. *Proc. 12th World Conference on Earthquake Engineering*.
5. Li, J., Samali, B., Ye, L. & Bakoss, S. (2002). Behaviour of concrete beam–column connections reinforced with hybrid FRP sheet. *Composite Structures*, Vol. 57, pp. 357–65.
6. Karayannis, C. G. & Sirkelis, G. M. (2008). Strengthening and rehabilitation of RC beam-column joints using carbon-FRP jacketing and epoxy resin injection. *Earthquake Engng. Struct. Dyn*., Vol. 37, pp. 769-790.
7. Ghobarah, A. & Said, A. (2002). Shear strengthening of beam-column joints. *Engineering Structures*, Vol. 24, No. 7, pp. 881-888.
8. Antonopoulos, C. P. & Triantafillou, T. C. (2002). Analysis of FRP-strengthened RC beam-column joints. *Journal of Composites for Construction*, Vol. 6, No. 1, pp. 41-51.
9. Antonopoulos, C. P. & Triantafillou, T. C. (2003). Experimental investigation of FRP-strengthened RC beam-column joints. *Composites for Construction*, Vol. 7-1, pp. 39-49.
10. Le-Trung, K., Lee, K., Lee, J., Lee, D. & Woo, S. (2010). Experimental study of RC beam-column joints strengthened using CFRP composites. *Composites, Part B: Engineering*, Vol. 41, No. 1, pp. 76-85.
11. Maheri, M. R. & Hadjipour, A. (2003). Experimental investigation and design of steel brace connection to RC frame. *Engineering Structures*, Vol. 25, No. 13, pp. 1707-1714.
12. Maheri, M. R. & Ghaffarzadeh, H. (2008). Connection overstrength in steel-braced RC frames. *Engineering Structures*, Vol. 30, No. 7, pp. 1938-1948.
13. Mahini, S. S. & Ronagh, H. R. (2007). A new method for improving ductility in existing RC ordinary moment resisting frames using FRPs. *Asian Journal of Civil Engineering (Building and Housing)*, Vol. 8, No. 6, pp. 581-595.
14. Smith, S. T. & Shrestha, R. (2006). A review of FRP strengthened RC beam column connections. *Proceedings of the Third International Conference on FRP Composites in Civil Engineering, Miami, Florida*, USA, pp. 661-664.

15. Robert Ravi, S. & Prince Arulraj, G. (2010). Experimental investigation on behaviour of reinforced concrete beam column joints retrofitted with GFRP-CFRP hybrid wrapping. *Int. J of Civil & Structural Engineering*, Vol. 1, No. 2, pp. 245-253.
16. Niroomandi, A., Maheri, A., Maheri, M. R. & Mahini, S. S. (2010). Seismic performance of ordinary RC frames retrofitted at joints by FRP sheets**.** *Engineering Structures*, Vol. 32, No. 8, pp. 2326-2336.
17. Maheri, M. R. & Akbari, R. (2003). Seismic behaviour factor, R, for steel X-braced and knee-braced RC buildings. *Engineering Structures*, Vol. 25, pp. 1505-1513.
18. Balsamo, A., Colombo, A., Manfredi, G., Negro, P. & Prota, A. (2005). Seismic behavior of a full scale RC frame repaired using CFRP laminates. *Engineering Structures*, Vol. 27, pp. 769-780.
19. Di Ludovico, M., Prota, A., Manfredi, G. & Cosenza, E. (2008). Seismic strengthening of an under-designed RC structure with FRP. *Earthquake Engng. Struct. Dyn*., Vol. 37, pp. 141-162.
20. ANSYS Manual, ANSYS, INC., Canonsburg, PA 15317, USA, (2005).
21. SAP2000 nonlinear version 10.1.0, (2006). *Analysis reference manual*. Computers and Structures Inc., Berkeley, California.
22. Chen, J. F. & Teng, J. G. (2001). Anchorage strength model for FRP and steel plates attached to concrete. *Journal of Structural Engineering*, ASCE, Vol. 127, No. 7, pp. 784-791.
23. ACI 440.2R-08, ACI Committee 440-02, (2008). Guide for the design and construction of externally bonded FRP system for strengthening concrete structures, MCP 2005, ACI, Michigan, USA.
24. ACI Committee 318, (1989). Building code requirements for reinforced concrete (ACI 318-95) and Commentary (ACI 318R-95). American Concrete Institute, Detroit, Michigan.
25. Mostofinejad D. & Talaeitaba, S. B. (2006). Finite element modelling of RC connections strengthened with FRP laminates. *Iranian Journal of Science and Technology, Transaction B: Engineering*, Vol. 30, No. B1, pp. 21-30.
26. Pauley, T. & Priestley, M. J. N. (1992). *Seismic design of reinforced concrete and masonry buildings*. John Wiley & Sons, Inc.
27. ATC, (1996). Seismic evaluation and retrofit of concrete buildings, ATC-40, Applied Technology Council, Redwood City.
28. American Society of Civil Engineering (ASCE), (2000). Prestandard and commentary for the seismic rehabilitation of buildings, Prepared for the Federal Emergency Management Agency, FEMA 356.
29. Mwafy, A. M. & Elnashai, A. S. (2002). Calibration of force reduction factors of RC buildings. *Journal of Earthquake Engineering*, Vol. 6, No. 2, pp. 239–73.
30. Nassar, A. A. & Krawinkler, H. (1991). Seismic demands for SDOF and MDOF systems, Report No. 95. Stanford, California: The John A. Blume Earthquake Engineering Center, Stanford University.
31. Federal Emergency Management Agency (FEMA), (1997). *NEHRP Provisions for the seismic rehabilitation of buildings, Report, FEMA 273 and 274*, Washington DC.
32. Iranian code of practice for seismic resistance design of buildings, Standard No. 2800, 2nd. Edition, (2005).